THE JOURNAL OF BIOLOGICAL CHEMISTRY
Vol. 274, No. 44, Issue of October 29, pp. 31679–31685, 1999
Printed in U.S.A.

Cloning and Sequencing of the Coenzyme B_{12}-binding Domain of Isobutyryl-CoA Mutase from *Streptomyces cinnamonensis*, Reconstitution of Mutase Activity, and Characterization of the Recombinant Enzyme Produced in *Escherichia coli**

(Received for publication, August 2, 1999)

Ananda Ratnatilleke, Jan W. Vrijbloed, and John A. Robinson‡

From the Institute of Organic Chemistry, University of Zurich, Winterthurerstrasse 190, 8057 Zurich, Switzerland

Isobutyryl-CoA mutase (ICM) catalyzes the reversible, coenzyme B_{12}-dependent rearrangement of isobutyryl-CoA to *n*-butyryl-CoA, which is similar to, but distinct from, that catalyzed by methylmalonyl-CoA mutase. ICM has been detected so far in a variety of aerobic and anaerobic bacteria, where it appears to play a key role in valine and fatty acid catabolism. ICM from *Streptomyces cinnamonensis* is composed of a large subunit (IcmA) of 62.5 kDa and a small subunit (IcmB) of 14.3 kDa. *icmB* encodes a protein of 136 residues with high sequence similarity to the cobalamin-binding domains of methylmalonyl-CoA mutase, glutamate mutase, methyleneglutarate mutase, and cobalamin-dependent methionine synthase, including a conserved DXHXXG cobalamin-binding motif. Using IcmA and IcmB produced separately in *Escherichia coli*, we show that IcmB is necessary and sufficient with IcmA and coenzyme B_{12} to afford the active ICM holoenzyme. The large subunit (IcmA) forms a tightly associated homodimer, whereas IcmB alone exists as a monomer. In the absence of coenzyme B_{12}, the association between IcmA and IcmB is weak. The ICM holoenzyme appears to comprise an $\alpha_2\beta_2$-heterotetramer with up to two molecules of bound coenzyme B_{12}. The equilibrium constant for the ICM reaction at 30 °C is 1.7 in favor of isobutyryl-CoA, and the pH optimum is near 7.4. The K_m values for isobutyryl-CoA, *n*-butyryl-CoA, and coenzyme B_{12} determined with an equimolar ratio of IcmA and IcmB are 57 ± 13, 54 ± 12, and 12 ± 2 μM, respectively. A V_{max} of 38 ± 3 units/mg IcmA and a k_{cat} of 39 ± 3 s^{-1} were determined under saturating molar ratios of IcmB to IcmA.

The coenzyme B_{12}-dependent isobutyryl-CoA mutase (ICM[1]; butanoyl-CoA:2-methylpropanoyl-CoA mutase, EC 5.4.99.13) catalyzes the reversible rearrangement of isobutyryl-CoA to *n*-butyryl-CoA. Although closely related to the well known and widely distributed methylmalonyl-CoA mutase (MCM) reaction (1) (Fig. 1), MCM does not catalyze the rearrangement of isobutyryl-CoA to *n*-butyryl-CoA (2, 3). ICM has been detected in several polyketide antibiotic-producing streptomycetes, where it appears to play a key role in valine and fatty acid catabolism as well as in the production of fatty acid-CoA thioester building blocks for polyketide antibiotic biosynthesis (4). In earlier work (5), purification of ICM from the monensin-producing microorganism *Streptomyces cinnamonensis* gave a protein (IcmA) of ~65 kDa whose gene was subsequently cloned and expressed in *Escherichia coli*. However, recombinant IcmA alone showed no ICM activity. Using IcmA with a His_6 tag attached to its N terminus, a second subunit of ICM with an apparent mass of ≈17 kDa as determined by SDS-polyacrylamide gel electrophoresis (denoted IcmB) was isolated by affinity chromatography from *S. cinnamonensis*, which gave ICM activity when combined with IcmA and coenzyme B_{12} (5). In this work, we describe for the first time the cloning and sequencing of the gene encoding IcmB and the first characterization of ICM reconstituted from small and large subunits produced separately in *E. coli*.

The MCMs from *S. cinnamonensis* (2) and *Propionibacterium shermanii* (6) are heterodimers with subunits of ≈79 kDa (MutB) and ≈65 kDa (MutA). Several crystal structures of *P. shermanii* MCM were reported recently (7–9), which revealed a single coenzyme B_{12} molecule bound to the 728-residue MutB protein, sandwiched between a $(\beta/\alpha)_8$-triosephosphate isomerase barrel and a C-terminal, flavodoxin-like, cobalamin-binding domain. IcmA from *S. cinnamonensis*, however, comprises only 566 residues (5), corresponding to a loss of the entire ≈160-residue C-terminal cobalamin-binding domain from MutB. The sequence of the $(\beta/\alpha)_8$-barrel in MutB comprising residues A1–A400 is highly conserved in IcmA. Residues A401–A559 in MutB correspond to a largely helical linker, which connects the $(\beta/\alpha)_8$-barrel with the cobalamin-binding domain (residues A560–A728). The linker residues A401–A559 correspond in a sequence alignment approximately with residues 393–560 in IcmA, although the sequence identity in this region is only ≈18%. But after just 6 more residues, IcmA terminates.

The structure determination of the cobalamin-binding domain of MetH, a member of the methyltransferase family, revealed for the first time a protein-bound form of methylcobalamin, a vitamin B_{12} derivative (10). The cobalamin was shown bound to the protein with a histidine residue providing an axial imidazole ligand to cobalt, replacing the DMB group appended to the corrin ring. This key histidine residue is found in the motif DXHXXG, which is conserved in some (but not all) of the coenzyme B_{12}-dependent mutases (11). The crystal structure of MCM from *P. shermanii* revealed not only an active site, inaccessible to solvent, embedded along the axis of the $(\beta/\alpha)_8$-barrel in MutB (7, 8), but also the coordination of cobalt in coenzyme B_{12} by the histidine in the conserved DXHXXG motif within the C-terminal cobalamin-binding domain. In the case

* This work was supported by the Swiss National Science Foundation and the Stipendium Commission of the Swiss Federal Government. The costs of publication of this article were defrayed in part by the payment of page charges. This article must therefore be hereby marked "*advertisement*" in accordance with 18 U.S.C. Section 1734 solely to indicate this fact.

The nucleotide sequence(s) reported in this paper has been submitted to the GenBank™/EBI Data Bank with accession number(s) AJ246005.

‡ To whom correspondence should be addressed. Tel.: 41-1-635-4242; Fax: 41-1-635-6812; E-mail: robinson@oci.unizh.ch.

[1] The abbreviations used are: ICM, isobutyryl-CoA mutase; MCM, methylmalonyl-CoA mutase; DMB, dimethylbenzimidazole; kb, kilobase pair(s); ORF, open reading frame.

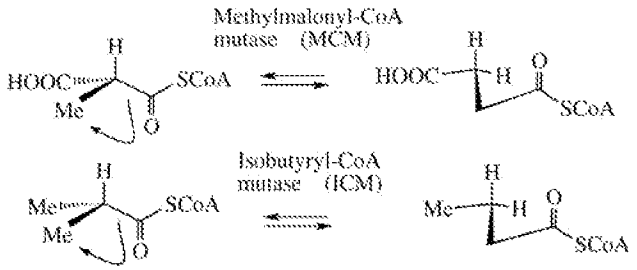

FIG. 1. **Reactions catalyzed by MCM and ICM.**

of ICM, however, the large subunit (IcmA) contains no contiguous cobalamin-binding domain, but instead requires a separate small subunit (IcmB) to bind coenzyme B_{12} and to afford active mutase (5). This suggested that IcmB has taken on the role of a separate cobalamin-binding domain in ICM, a conclusion that is confirmed here by the high sequence similarity between IcmB and the cobalamin-binding domains of MutB, methyleneglutarate mutase, and MetH as well as the small subunit (MutS) of glutamate mutase.

EXPERIMENTAL PROCEDURES

Bacterial Strains—*S. cinnamonensis* A3823.5, a high-yield producer of monensin A, was a gift of Lilly. *E. coli* BL21(DE3) pLysS (12) was purchased from Novagen.

Production of IcmA and Assay—IcmA was produced in *E. coli* BL21 pLysS[pET3a-*icmA*] as described earlier (5). The ICM assay was as described earlier (2). Briefly, *n*-butyryl-CoA (or isobutyryl-CoA; 280 μM final concentration) was added to an assay mixture containing 50 μM coenzyme B_{12}, 50 mM potassium phosphate (pH 7.4), and IcmA and IcmB. The reaction was incubated in the dark at 30 °C, typically until 10–15% conversion of substrate to product, and then stopped by addition of 100 μl of 2 M KOH containing 0.002% (v/v) *n*-valeric acid. After acidifying with 100 μl of 15% (v/v) H_2SO_4 and saturating with NaCl, the solution was extracted with EtOAc. The extract was analyzed directly by gas chromatography using a FFAP capillary column (10 m × 0.53 mm; Hewlett-Packard Co.).

Purification of IcmB—IcmB was purified from both *S. cinnamonensis* and *Streptomyces lividans* TK64 as described earlier (5). The N-terminal amino acid sequences of both proteins were determined by the Edman method using an automated sequencer. The N-terminal sequences obtained were as follows: *S. lividans*, GVAAGPIRVVVAKPGLDGHD; and *S. cinnamonensis*, GVAAGPIRVVVAKPGLDGHDRGAKVIARAL.

Cloning icmB—General DNA manipulations were performed in *E. coli* (13) and *Streptomyces* (14) as described. Two oligonucleotides were designed based on the N-terminal protein sequence of IcmB (S = G and C) (Oligo-1 and -2).

```
V   A   K   P   G   L   D   G   H   D
GTS GCS AAG CCS GGS CTS GAC GGS CAC GAC
```

OLIGO-1

```
D   G   H   D   R   G   A   K   V   I
GAC GGS CAC GAC CGS GGS GCS AAG GTS ATC
```

OLIGO-2

S. cinnamonensis genomic DNA digested with the restriction enzyme *Sal*I was shown by Southern blotting to contain fragments of ~1.65 kb that hybridized to both oligonucleotide probes. DNA fragments in the size range 1.6–1.8 kb were isolated from *Sal*I-digested genomic DNA and ligated into *Sal*I-cut pUC18 (15). A clone was isolated from this library using Oligo-1 as a probe. This clone (pOCI706) contained an ≈1.65-kb DNA insert, which was sequenced on both DNA strands by the dideoxy method using dye terminator chemistry (Perkin-Elmer). The GCG Version 8.1-unix software package (Genetics Computer Group, Madison, WI) (16) was used for sequence analysis. The sequence is shown in Fig. 2.

Expression of icmB—The 411-base pair *icmB* gene was amplified by polymerase chain reaction using the following oligonucleotides as primers and pOCI706 DNA as template: ICMBFOR, AGTCATCATATGGGTGTGGCAGCCGGGCCGATCC; and ICMBBACK, ATCATGGATCCTCAGACGGCCTGTCGCACGTTCC. The *Nde*I and *Bam*HI restriction sites in the primers are underlined. After polymerase chain reaction, the product was digested with *Nde*I and *Bam*HI and ligated between the corresponding restriction sites in pET3a (12). The resulting plasmid (pOCI711) was introduced into *E. coli* BL21(DE3) pLysS for production of IcmB.

Cells containing pOCI711 were grown in 2 × 20 ml of LB medium containing ampicillin (50 μg/ml) and chloramphenicol (34 μg/ml) to $A_{600\,nm} \approx 0.7$ at 30 °C. The cells from this preculture were used to inoculate 8 × 500 ml of 2YT medium (Difco) containing ampicillin and chloramphenicol. The cells were grown to $A_{600\,nm} \approx 0.6$ with shaking at 200 rpm and 30 °C. Protein expression was induced with isopropyl-β-D-thiogalactopyranoside to a final concentration of 0.3 mM and shaken for an additional 4 h. The cells were harvested by centrifugation at 4 °C and stored at −20 °C.

The cell pellet from 1.5 liters of culture was sonicated in buffer A (50 mM Tris-HCl (pH 7.5), 5 mM EDTA, 1 mM benzamidine, 1 mM phenylmethanesulfonyl fluoride, 1 mM dithiothreitol, 0.1% (v/v) 2-mercaptoethanol, and 5% (v/v) glycerol). The cell-free extract (~35 mg of protein) was applied to a Q-Sepharose column (1.5 × 7 cm; Fast flow, Amersham Pharmacia Biotech) equilibrated with buffer B (50 mM Tris-HCl (pH 7.5) and 5 mM EDTA). The column was washed with 20 column volumes of buffer B and then eluted at a flow rate of 3 ml/min with a linear gradient of 0–1 M KCl in buffer B over 100 ml. The fraction containing IcmB eluted in the range 100–350 mM KCl as detected by an ICM activity assay. The ICM-active fractions were pooled (20 mg of protein) and dialyzed against buffer C (50 mM Tris-HCl (pH 7.5) and 0.5 mM EDTA) containing 1 mM dithiothreitol.

The dialyzed sample (18 mg of protein) was applied to a MonoQ column (HR 5/5, Amersham Pharmacia Biotech) equilibrated with buffer C. The column was washed with 50 column volumes of buffer C and then eluted at a flow rate of 1.5 ml/min using a 0–1 M KCl gradient in buffer C over 100 ml. The fractions eluting between 90 and 200 mM KCl possessed the highest ICM activity and were pooled and dialyzed against buffer C (yield of 5 mg of protein).

The dialyzed sample (4.5 mg of protein) from above was rechromatographed on the MonoQ column under the same conditions as described above. IcmB eluted as a single peak (yield of 0.5 mg of protein) at 200 mM KCl and was homogeneous as determined by SDS-polyacrylamide gel electrophoresis (see Fig. 4). The protein was dialyzed against 50 mM potassium phosphate (pH 7.5) containing 1 mM dithiothreitol and stored at 4 °C. IcmB can be stored in this way for several weeks without significant loss of activity.

Characterization of IcmA and IcmB—Native molecular masses were determined by gel filtration chromatography (Superose 12 HR 10/26 column, Amersham Pharmacia Biotech) in buffer D (50 mM potassium phosphate (pH 7.4), 150 mM KCl, and 0.5 mM EDTA). Standards for molecular mass calibration were blue dextran (2000 kDa), catalase (232 kDa), aldolase (158 kDa), bovine serum albumin (67 kDa), and ribonuclease A (13.6 kDa). The extinction coefficients of IcmA and IcmB at 280 nm were determined using the Beer-Lambert law and quantitative amino acid analysis for determination of protein concentrations: ϵ_{280} = 122,000 ± 12,000 for IcmA and ϵ_{280} = 10,280 ± 2100 for IcmB. Each measurement was carried out in triplicate, and the means ± S.D. are given. The protein concentrations determined in this way were in good agreement with those from Bradford assays (17). The molecular mass of recombinant IcmB in deionized water was determined by mass spectrometry using an ion-spray source.

Equilibrium Constant Determination—The equilibrium constant for the ICM reaction at pH 7.4 and 30 °C was obtained by determining the equilibrium concentrations of both *n*-butyryl-CoA and isobutyryl-CoA. Assays contained 25 nM IcmA, 25 nM IcmB, and 0.1 mM coenzyme B_{12} in 3.2 ml of 50 mM potassium phosphate buffer (pH 7.4) equilibrated at 30 °C. *n*-Butyryl-CoA or isobutyryl-CoA (140 μM) was added to start the reaction; and periodically, samples were taken to determine the ratio of isobutyryl-CoA to *n*-butyryl-CoA. This experiment was then repeated using 10 different starting ratios of *n*-butyryl-CoA to isobutyryl-CoA (ratios in the range 0.4–2.1) roughly in the range of the estimated equilibrium constant determined above. The equilibrium constant for the ICM reaction was obtained by plotting the change in [isobutyryl-CoA] *versus* the [isobutyryl-CoA]/[*n*-butyryl-CoA] ratio. This gave K_{eq} = 1.7 ± 0.05 in favor of isobutyryl-CoA.

Kinetic Analyses—For determination of K_m and V_{max} values, initial velocities were determined using the gas chromatography assay (see above) in 50 mM potassium phosphate buffer (pH 7.4) at 30 °C. For the measurement of K_m values, IcmA and IcmB (each at 5 nM) were used in a 1:1 molar ratio. The conversion of substrate to product was followed by withdrawing samples from the assay mixture (typically five time points for each assay) up to a maximum of 10–15% conversion, and these data were used to calculate initial rates. Typically, six different substrate

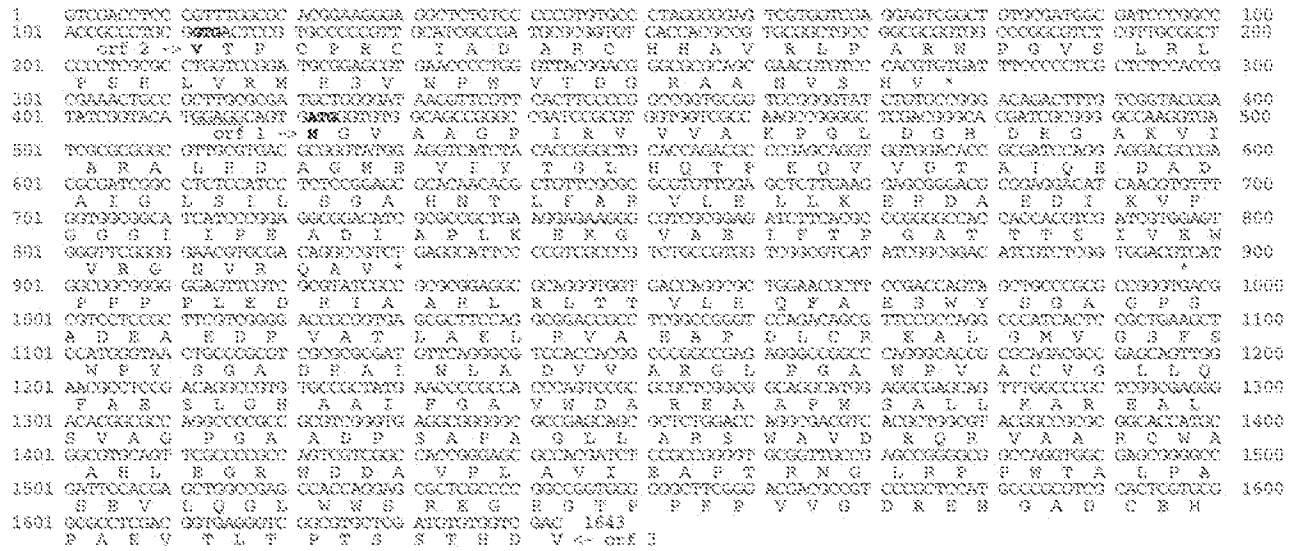

FIG. 2. **Nucleotide sequence of the cloned DNA from *S. cinnamonensis*.** The location of ORFs predicted from a FRAME analysis are shown. ORF3 is encoded on the opposite strand (not shown). The other ORFs are encoded on the DNA strand shown, and the amino acid sequence in each ORF is given below the nucleotide sequence. The predicted start codons are shown in *boldface*. The predicted ribosome-binding site for ORF1 (*icmB*) is *underlined*.

concentrations were used in the range 13.3–200 μM for *n*-butyryl-CoA and 13.3–300 μM for isobutyryl-CoA. At each fixed substrate concentration, assays were performed with five different coenzyme B_{12} concentrations in the range 4.8–200 μM. All measurements were carried out in triplicate, and the S.D. in K_m values was approximately ±25% (see Table II).

The general form of the rate equation for a bireactant mechanism is represented by Equation 1,

$$v = V_{max}[A][B]/(K_{i(A)}K_{m(B)} + K_{m(A)}[B] + K_{m(B)}[A] + [A][B]) \quad \text{(Eq. 1)}$$

where v, V_{max}, [A], and [B] are the initial velocity, maximum velocity, and concentrations of the first substrate A and second substrate B, respectively (18). $K_{m(A)}$, $K_{m(B)}$, and $K_{i(A)}$ are the Michaelis constants for substrates A and B and the dissociation constant for the first substrate A, respectively. The initial velocity data were fitted to Equation 1 using the computer program Leonora Version 1.0 (19, 20) (see Fig. 7, *A* and *B*).

The V_{max} was determined from a Hanes plot (see Fig. 7*C*) using saturating amounts of IcmB (75 nM) relative to IcmA (5 nM), at six different *n*-butyryl-CoA concentrations in the range 40–1000 μM, and at a coenzyme B_{12} concentration of 0.2 mM.

The Hill constant (h) was measured by varying the IcmB concentration (1–75 nM) at one fixed concentration of IcmA (5 nM) and fitting initial rates to the following form of the Hill equation (Equation 2),

$$\log_{10}v/(V_{max} - v) = h \times \log_{10}[\text{IcmB}] \quad \text{(Eq. 2)}$$

RESULTS

Sequence and Expression of icmB—The 1.65 kb of *S. cinnamonensis* genomic DNA, isolated from a library using oligonucleotides encoding the N terminus of IcmB, were sequenced and analyzed using CODONPREFERENCE in the GCG software (16). This revealed two complete ORFs (ORF1 and ORF2) and one (ORF3) with incomplete sequence data (Fig. 3). ORF1, starting at nucleotide 422 and ending at nucleotide 832, was identified as the *icmB* gene, encoding a protein of 136 residues with a mass of 14,333 Da. The putative ORF2, immediately upstream of ORF1, encodes a protein of only 55 residues and, like ORF3, lacks significant similarity to proteins in the EBI/Swiss Protein Data Bank. The deduced amino acid sequence of IcmB shows significant identity to several cobalamin-dependent proteins in the data base, as shown in Table I.

To produce IcmB in *E. coli*, *Nde*I and *Bam*HI sites were introduced at the 5′- and 3′-ends of *icmB* such that the *Nde*I site encodes an ATG start codon, and the gene was cloned in the expression vector pET3a (12). After introduction into *E. coli* BL21(DE3) pLysS, the production of active IcmB could be detected in cell extracts in an assay with IcmA and coenzyme B_{12}. After isolation by standard methods (see "Experimental Procedures"), the protein was homogeneous as determined by SDS-polyacrylamide gel electrophoresis (Fig. 4), with an apparent mass of ~17 kDa, as observed in earlier work (5). An electrospray mass spectrum of IcmB gave a molecular ion with a mass of 14,203 Da, consistent with the deduced protein sequence minus methionine.

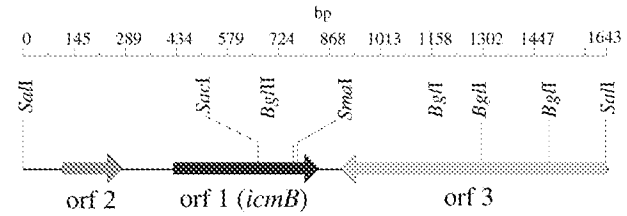

FIG. 3. **Organization of ORFs predicted by a FRAME analysis using CODONPREFERENCE in the GCG software (16).** See "Results".

TABLE I

Protein sequence identities and similarities between IcmB from S. cinnamonensis and the small subunit (MutS) of glutamate mutase from C. tetanomorphum, the small subunit (GlmS) of glutamate mutase from Clostridium cochlearium, the large subunit of MCM (MutB) from S. cinnamonensis, MutB from P. shermanii, methyleneglutarate mutase from C. barkeri, MetH from E. coli, the MCM-like small protein from P. horikoshii, and the MCM-like small protein from A. fulgidus (GAP, GCG software, Gap Weight 3.0) and their corresponding peptide chain lengths

Protein sequence	Identity	Similarity	Chain length
	%	%	
MutS of GM[a] (*C. tetanomorphum*)	24	48	137
GlmS of GM (*C. cochlearium*)	24	49	137
MutB of MCM			
S. cinnamonensis	37	60	733
P. shermanii	40	58	728
MGM (*C. barkeri*)	37	57	614
MetH (*E. coli*)	22	50	1227
MCM-like small protein			
P. horikoshii	56	73	147
A. fulgidus	56	76	144

[a] GM, glutamate mutase; MGM, methyleneglutarate mutase.

Characterization of ICM—Upon gel filtration chromatography, IcmB eluted with an apparent mass of 17 kDa, suggesting

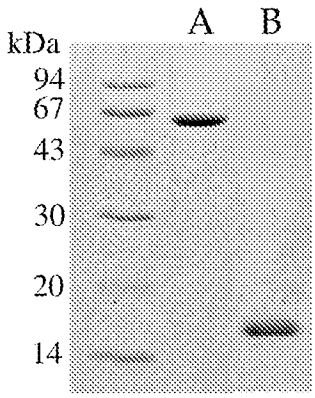

FIG. 4. **Coomassie Blue-stained SDS-polyacrylamide gel (20% homogeneous) of purified recombinant IcmA (*lane A*) and IcmB (*lane B*).** Molecular mass standards are shown.

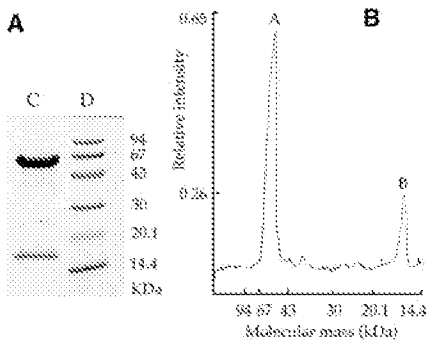

FIG. 5. **Coomassie Blue-stained SDS-polyacrylamide gel showing the IcmA and IcmB subunits of the protein complex corresponding to a mass of ~152 kDa (*lane C*) (size markers are indicated in *lane D*) eluted as a single peak from a gel filtration column in the presence of coenzyme B_{12} (*A*) and plot of the relative densitometric intensities of the IcmA and IcmB protein bands on the gel (as in *A*) *versus* the molecular mass (*B*).**

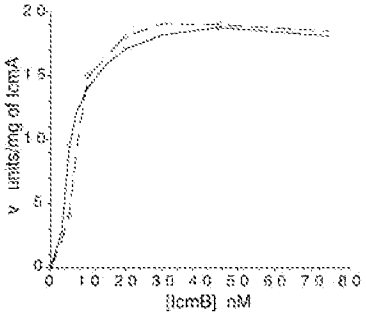

FIG. 6. **Plots of initial velocity of ICM *versus* IcmB concentration at a fixed concentration of IcmA (5 nM).** The *two curves* represent experimental data from two independent measurements.

a largely monomeric protein. Under the same conditions, IcmA eluted from the column with an apparent mass of 135 kDa, almost double the calculated mass of 62.5 kDa, indicating a homodimer. Gel filtration of a 1:1 molar ratio of IcmA to IcmB led to the elution of the two subunits separately from the column at the expected apparent masses. When IcmA and IcmB were first incubated with coenzyme B_{12}, a single major peak eluted from the gel filtration column with an apparent mass of ≈152 kDa. This peak showed a UV spectrum with λ_{max} at 522 and 375 nm, characteristic of enzyme-bound coenzyme B_{12}, and high ICM activity (3.3 μmol/min/mg). As determined by SDS-polyacrylamide gel electrophoresis, this peak showed bands corresponding to both IcmA and IcmB and, as determined by densitometric scanning, in almost exactly a 1:1 molar ratio (Fig. 5). This indicates a likely $\alpha_2\beta_2$-quaternary structure for native ICM with bound coenzyme B_{12}. The pH optimum for the ICM reaction was ~7.4, and the activity diminished only slightly at pH 6.0 and 8.0.

Kinetics—The steady-state kinetic properties of the enzyme were investigated. The two subunits and coenzyme B_{12} are necessary and sufficient to observe ICM activity with *n*-butyryl-CoA or isobutyryl-CoA as substrate. The specific activity of the enzyme was seen to vary with the molar ratio of IcmA to IcmB in the assay. The activity approached saturation only after a severalfold molar excess of IcmB to IcmA was present (Fig. 6). The plot of activity against IcmB concentration appeared slightly sigmoidal, suggestive of some degree of cooperativity in formation of the holoenzyme from IcmA, IcmB, and coenzyme B_{12}. Fitting the velocity data to Equation 2 gave a Hill coefficient of 1.34 ± 0.02.

Under the standard assay conditions, as used during the earlier purification of IcmA (5), the specific activity of the enzyme in the presence of a 1:1 molar ratio of IcmA to IcmB was ~8.0 μmol/min/mg. In the earlier work (5), after partial purification of IcmA from extracts of *S. cinnamonensis*, the specific activity was ~0.023 μmol/min/mg, and after reconstitution of mutase from recombinant His_6-IcmA and IcmB isolated from *S. cinnamonensis*, it was ~1.0 μmol/min/mg.

For the determination of K_m values, the initial rates were typically measured at six different substrate concentrations in the range 13.3–200 μM, and for each fixed concentration of substrate, rates were typically determined at five different coenzyme B_{12} concentrations between 4.8 and 200 μM. A 1:1 molar ratio of IcmA to IcmB was used throughout. The data were fitted to Equation 1 by nonlinear least-squares regression using the computer program Leonora Version 1.0 (Fig. 7, *A* and *B*). The apparent K_m values determined were 54 ± 12 μM for *n*-butyryl-CoA, 57 ± 13 μM for isobutyryl-CoA, and 12 ± 2 μM for coenzyme B_{12}. The V_{max} was determined to be 38 ± 5 units/mg IcmA from a Hanes plot (Fig. 7*C*) using varying concentrations of *n*-butyryl-CoA and saturating amounts of IcmB (15-fold molar excess compared with IcmA). Assuming one active site per IcmA monomer, k_{cat} = 39 ± 3 s^{-1} at saturating concentrations of IcmB.

DISCUSSION

icmA and *icmB* are not adjacent in the chromosome of *S. cinnamonensis*. In contrast, *mutA* and *mutB* from this organism share overlapping start and stop codons (2), a device that may lead to transcriptional coupling and hence to the production of stoichiometric amounts of the two proteins. It is presently unclear how far apart *icmA* and *icmB* are in the *S. cinnamonensis* genome, although the regions extending over 8 kb upstream and 11 kb downstream of *icmA*, isolated in an earlier work (5), do not contain sequences similar to *icmB*. Two hyperthermophilic bacteria, *Archeoglobus fulgidus* (21) and *Pyrococcus horikoshii* (22), whose genomes have now been completely sequenced, each contain two ORFs of similar size and sequence to *icmA* and *icmB*, although they were reported as MCM-like sequences. *mcmA1* and *mcmA2* from *A. fulgidus* encode proteins of 548 and 144 residues and are located only 2.5 kb apart, whereas the large and small ICM-like genes in *P. horikoshii* encode proteins of 563 and 147 residues, but are located ~230 kb apart. It is interesting to speculate that, in both organisms, these MCM-like proteins might be components of ICM. However, this remains to be proven. The distinguishing features of ICM include an MCM-like large subunit of only ~65 kDa, with a separate small subunit of ~14 kDa providing the cobalamin-binding domain. An isolated report has appeared of a propionate-induced MCM from *Euglena gracilis* that contains two mutases with apparent molecular masses of 72,000 and 17,000 Da (23). Neither protein, however, has yet been purified to homogeneity.

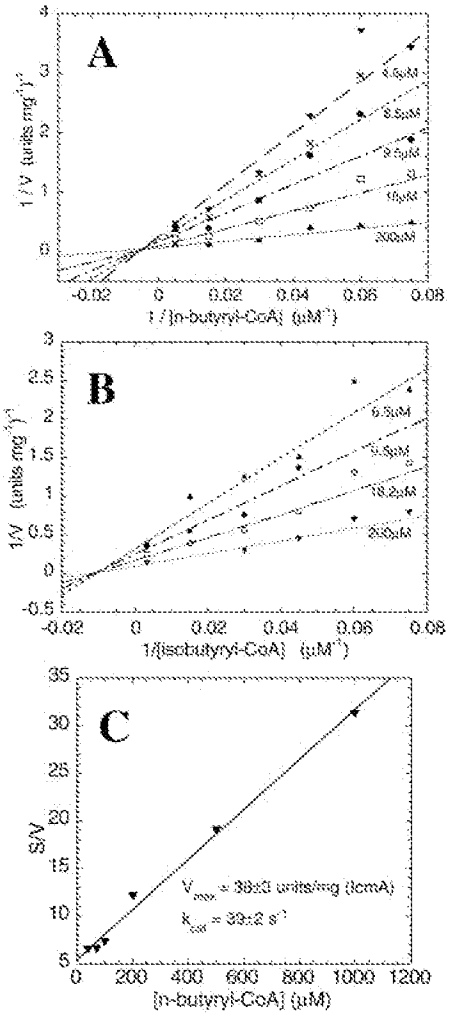

FIG. 7. *A* and *B*, double-reciprocal plots of 1/initial velocities (v) *versus* 1/substrate concentration for *n*-butyryl-CoA and isobutyryl-CoA, respectively, as substrate. The experimental data points are shown together with the best fit lines generated by the program Leonora after fitting to Equation 1. The coenzyme B_{12} concentration was varied between 4.8 and 200 μM or between 6.5 and 200 μM, as indicated on each plot. All measurements were repeated in triplicate for determination of K_m values. In *C*, a Hanes plot is shown with initial velocities (v) and *n*-butyryl-CoA concentration and with saturating coenzyme B_{12} (200 μM), as used to determine V_{max} and k_{cat} (see "Results").

Although in MCM a single polypeptide chain comprises both the coenzyme B_{12}- and substrate-binding domains, the glutamate mutase from clostridia consists of two subunits, MutE (which forms a tightly associated homodimer) and MutS (which is the coenzyme B_{12}-binding domain). The active glutamate mutase holoenzyme appears to be an $\alpha_2\beta_2$-heterotetramer that binds up to two molecules of coenzyme B_{12}, as deduced here for ICM.

The analysis of the kinetics for ICM is complicated by the fact that IcmA and IcmB interact only weakly until coenzyme B_{12} is added, and then IcmA binds to IcmB in a cooperative manner. This also complicates any attempts to measure the stoichiometry of bound coenzyme B_{12}. As a result, the apparent kinetic parameters depend on the relative concentrations of the two subunits, as observed earlier in studies of glutamate mutase (24, 25). Here, the substrate K_m values with ICM were determined using equimolar ratios of IcmA and IcmB, and the V_{max} was determined relative to the IcmA concentration at saturating concentrations of IcmB.

The assay used for the determination of kinetic constants is a discontinuous gas chromatography assay, which is not well suited for accurate initial velocity measurements. Notwithstanding this, in the determination of K_m values, a nonlinear least-squares regression fitting of the initial velocities to a velocity equation for a bireactant system converged for both substrates. Double-reciprocal plots gave sets of lines that intersected on or close to the x axis (Fig. 7, *A* and *B*). The results are consistent with either a random or ordered sequential mechanism, involving the reversible formation of a ternary complex between enzyme, substrate, and coenzyme B_{12}. The k_{cat} value of 39 ± 3 s^{-1} determined for ICM (Fig. 7*C*) assumes one active site per IcmA monomer subunit.

TABLE II
Apparent K_m and k_{cat} values for ICM determined in this work compared with values for glutamate mutase (24) and MCM (1, 26, 28) determined elsewhere

Enzyme (source)	Substrate/coenzyme	k_{cat}	K_m	k_{cat}/K_m
		s^{-1}	μM	$s^{-1}\,M^{-1}$
ICM	*n*-Butyryl-CoA	39 ± 3	54 ± 12	7.2×10^5
(*S.cinnamonensis*)	Isobutyryl-CoA		57 ± 13	
	Coenzyme B_{12}		12 ± 2	
GM[a]	Glutamate	20.6	1090	1.9×10^4
(*C. tetanomorphum*)	Coenzyme B_{12}		18.0	
MCM (*P. shermanii*)	Succinyl-CoA	48	96	5×10^5
	Methylmalonyl-CoA		80	
	Coenzyme B_{12}		0.035	

[a] GM, glutamate mutase.

The apparent K_m values for *n*-butyryl-CoA and isobutyryl-CoA are in the same range as the K_m values reported elsewhere for methylmalonyl-CoA and succinyl-CoA with MCM (26), but are at least an order of magnitude lower than the apparent K_m for glutamate with glutamate mutase, measured under comparable conditions (1:1 molar ratio of MutE to MutS) (Table II). It is interesting to note that MCM and ICM have similar substrate structures and most likely similar substrate-binding sites in their large subunits (see below), reflecting the similar K_m values for their substrates. On the other hand, ICM and glutamate mutase share a similar mode of cobalamin binding involving two independent subunits and have similar K_m values for coenzyme B_{12}. In comparison, a significantly lower K_m is found for coenzyme B_{12} with MCM (Table II).

Early insights into the structures of cobalamin-dependent enzymes came from a primary sequence comparison between the C-terminal domains (now also known as α/β-domains) of MetH and MCM (from both prokaryotic and eukaryotic organisms) with MutS of bacterial glutamate mutase (11). This revealed a region of highly conserved sequence comprising the motif **D*X*H*XX*G** (where *X* is any amino acid), which was invariant in all the proteins examined. After the determination of the crystal structure of the cobalamin-binding fragment of MetH, Drennen *et al.* (10) were able to define a sequence fingerprint for cobalamin binding that included $\mathbf{D^{757}}\mathit{X}\mathbf{H}\mathit{XX}\mathbf{G}\ldots\mathbf{S^{804}}\mathit{X}\mathbf{L}\ldots\mathbf{G^{833}G}$. This fingerprint is also apparent in IcmB (Fig. 8).

A notable feature in the crystal structures of both the cobalamin-binding fragment of MetH from *E. coli* (10) and MCM from *P. shermanii* (7) is the replacement of the DMB ligand from cobalt of the coenzyme by the histidine residue in the **D*X*H*XX*G** motif. The protein brings the cobalamin cofactor to a base-off/His-on form and places the DMB group in a central hydrophobic cleft in the cobalamin-binding domain. The histidine participates in a hydrogen-bonding network comprising 3 residues: His^{759}–Asp^{757}–Ser^{810} in MetH and His^{610}–Asp^{608}–Lys^{604} in MCM. In the case of IcmB, the corresponding residues appear to be well conserved and are represented by His^{20}–Asp^{18}–Lys^{14}, which most likely are also involved in binding coenzyme B_{12}. The other residues in the fingerprint sequence appear to line the hydrophobic cleft, to interact with the dis-

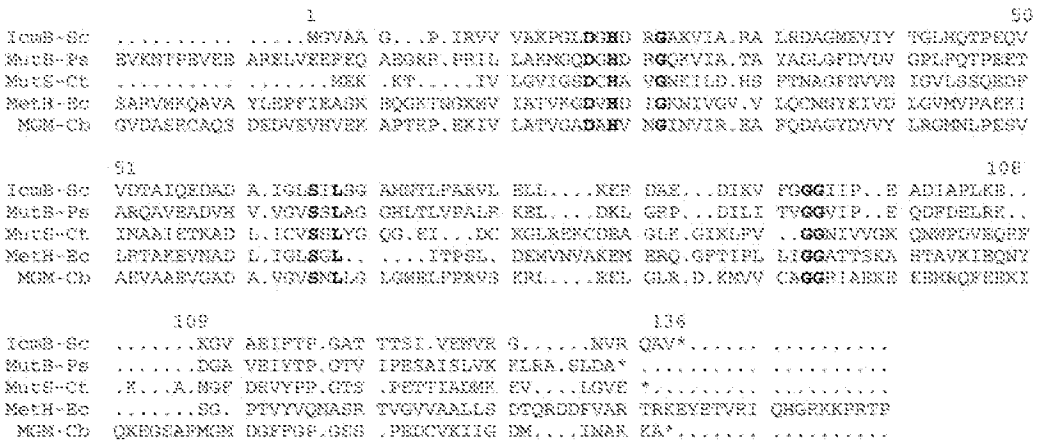

FIG. 8. **Alignment of deduced amino acid sequences of a subset of cobalamin-dependent enzymes with homologies to the α/β-domain of IcmB.** The sequences shown are as follows: residues 1–136 of IcmB from *S. cinnamonensis* (*IcmB-Sc*), residues 572–727 of MCM MutB from *P. shermanii* (*MutB-Ps*), residues 1–137 of glutamate mutase MutS from *Clostridium tetanomorphum* (*MutS-Ct*), residues 720–902 of MetH from *E. coli* (*MetH-Ec*), and residues 448–614 of methyleneglutarate mutase from *Clostridium barkeri* (*MGM-Cb*). The fingerprint sequence (10) is in *boldface*.

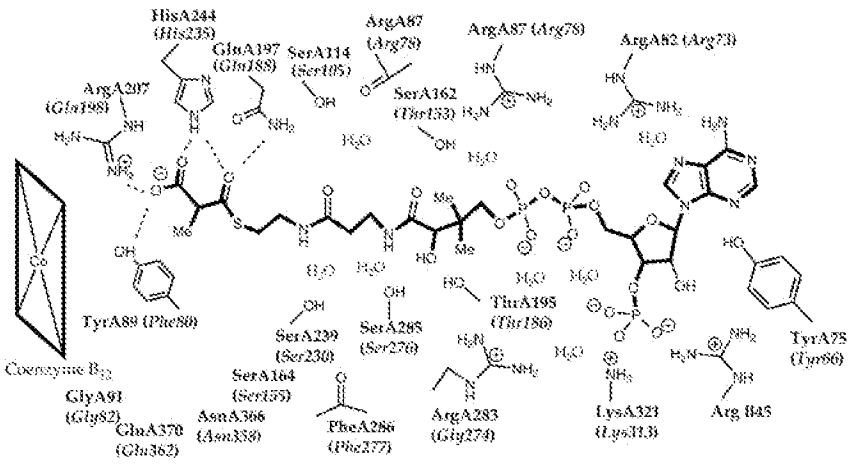

FIG. 9. **Schematic diagram showing the relative location of residues in MCM lining the substrate-binding site, together with the substrate methylmalonyl-CoA (taken from Refs. 7 and 9).** The residues are denoted by type, chain (A-chain = MutB and B-chain = MutA), and number. The corresponding residues in a sequence alignment (5) with IcmA are shown in each case in *parentheses* and in *italics*. Notable is the exchange of Arg^{A207} in MCM for Gln^{198} in IcmA (see "Discussion").

placed DMB group, and thereby to anchor the cobalamin molecule to the protein. These comparisons therefore suggest that the residues contacting the lower face of the corrin ring are conserved in IcmB and these other cobalamin-binding proteins.

The structural conservation of the cobalamin-binding domain is readily apparent from the available crystal structures of MetH and MCM as well as the NMR solution structure of MutS (27). The tertiary structures of the cobalamin-binding domains in MCM and MetH are essentially superimposable (7). The core structure consists of a five-stranded twisted parallel β-sheet surrounded by five α-helixes. The NMR solution structure of the coenzyme B_{12}-free form of MutS also revealed a similar tertiary structure (27), except for the first α-helix, which in solution appeared slightly disordered. The displacement of the DMB group of coenzyme B_{12} upon binding to the cobalamin-binding domain appears to be a common feature of several (but not all) coenzyme B_{12}-dependent mutases.

As shown in earlier work (5), the sequence of the $(\beta/\alpha)_8$-barrel in MutB comprising residues A1–A400 (7) is highly conserved in IcmA. This suggests that the triosephosphate isomerase barrel and much of the acyl-CoA-binding site identified in the crystal structure of MutB are also conserved in IcmA. The triosephosphate isomerase barrel uses a hole through its center to bind substrate, but also appears to open in the absence of ligand (8). Many of the residues that interact with CoA along the hole seem to be highly conserved in a sequence comparison with IcmA (Fig. 9). One residue, Tyr^{A89} in MutB, is conserved in all MCM sequences and is located near the bottom of the substrate-binding hole near to the interface with coenzyme B_{12}. A Y89F mutant of MCM was prepared recently, and its structure was determined by crystallography (28). Although the mutant enzyme structure was essentially superimposable on the wild-type structure and the K_m for succinyl-CoA was not significantly affected, the k_{cat} of the mutant was 580-fold lower than that of the wild type. Hence, it was suggested that Tyr^{A89} plays a key role in the MCM reaction, although not as a site for a protein-based radical. In the sequence comparison with IcmA (5), this Tyr^{A89} residue corresponds to Phe^{80}, so the hydrogen-bonding ability of a Tyr-OH is not needed at this site in ICM. The k_{cat} values for ICM and wild-type MCM are very similar (Table II).

Very recently, a crystal structure of MCM with bound substrate revealed an interaction between Arg^{A207} and the carboxyl group of methylmalonyl-CoA (9). As far as the different substrate specificities of MCM and ICM are concerned, it is intriguing to note that this Arg^{A207} residue is replaced in IcmA by a glutamine, whereas many other residues around the active site are highly conserved between MutB and IcmA (Fig. 9). Presently, it seems reasonable to assume that the catalytic mechanisms of ICM and MCM will be largely similar or identical.

Acknowledgment—We thank Annelies Meier for expert technical assistance.

REFERENCES

1. Rétey, J. (1982) in *B12* (Dolphin, D., ed) Vol. 2, pp. 357–379, John Wiley & Sons, Inc., New York
2. Birch, A., Leiser, A., and Robinson, J. A. (1993) *J. Bacteriol.* **175,** 3511–3519
3. Brendelberger, G., Retey, J., Ashworth, D. M., Reynolds, K., Willenbrock, F., and Robinson, J. A. (1988) *Angew. Chem. Int. Ed. Engl.* **27,** 1089–1090
4. Reynolds, K. A., O'Hagan, D., Gani, D., and Robinson, J. A. (1988) *J. Chem. Soc. Perkin Trans. I* 3195–3207
5. Zerbe-Burkhardt, K., Ratnatilleke, A., Philippon, N., Birch, A., Leiser, A., Vrijbloed, J. W., Hess, D., Hunziker, P., and Robinson, J. A. (1998) *J. Biol. Chem.* **273,** 6508–6517
6. Marsh, E. N., McKie, N., Davis, N. K., and Leadlay, P. F. (1989) *Biochem. J.* **260,** 345–352
7. Mancia, F., Keep, N. H., Nakagawa, A., Leadlay, P. F., McSweeney, S., Rasmussen, B., Bösecke, P., Diat, O., and Evans, P. R. (1996) *Structure* **4,** 339–350
8. Mancia, F., and Evans, P. R. (1998) *Structure* **6,** 711–720
9. Mancia, F., Smith, G. A., and Evans, P. R. (1999) *Biochemistry* **38,** 7999–8005
10. Drennan, C. L., Huang, S., Drummond, J. T., Matthews, R. G., and Ludwig, M. L. (1994) *Science* **266,** 1669–1674
11. Marsh, E. N. G., and Holloway, D. E. (1992) *FEBS Lett.* **310,** 167–170
12. Studier, F. W., Rosenberg, A. H., Dunn, J. J., and Dubendorff, J. W. (1990) *Methods Enzymol.* **185,** 60–89
13. Ausubel, F. M., Brent, R., Kingston, R. E., Moore, D. D., Seidman, J. G., Smith, J. A., and Struhl, K. (eds) (1987) *Current Protocols in Molecular Biology*, John Wiley & Sons, Inc., New York
14. Hopwood, D. A., Bibb, M. J., Chater, K. F., Kieser, T., Bruton, C. J., Kieser, H. M., Lydiate, D. J., Smith, C. P., Ward, J. M., and Schrempf, H. (1985) *Genetic Manipulation of Streptomyces: A Laboratory Manual*, The John Innes Institute, Norwich, England
15. Norrander, J., Kempe, T., and Messing, J. (1983) *Gene (Amst.)* **26,** 101–106
16. Devereux, J., Haeberli, P., and Smithies, O. (1984) *Nucleic Acids Res.* **12,** 387–395
17. Bradford, M. M. (1976) *Anal. Biochem.* **72,** 248–254
18. Segel, I. H. (1993) *Enzyme Kinetics: Behavior and Analysis of Rapid Equilibrium and Steady-state Enzyme Systems*, John Wiley & Sons, Inc., New York
19. Cornish-Bowden, A. (1994) *Leonora, a Computer Program: Steady State Kinetics on the IBM*, Oxford University Press, New York
20. Cornish-Bowden, A. (1995) *Analysis of Enzyme Kinetic Data*, Oxford University Press, New York
21. Klenk, H. P., Clayton, R. A., (J. F., T., O., W., K. E., N., K. A., K., R. J., D.,) Gwinn, M., Hickey, E. K., Peterson, J. D., Richardson, D. L., Kerlavage, A. R., Graham, D. E., Kyrpides, N. C., Fleischmann, R. D., Quackenbush, J., Lee, N. H., Sutton, G. G., Gill, S., Kirkness, E. F., Dougherty, B. A., McKenney, K., Adams, M. D., Loftus, B., and Venter, J. C. (1997) *Nature* **390,** 364–370
22. Kawarabayasi, Y., Sawada, M., Horikawa, H., Haikawa, Y., Hino, Y., Yamamoto, S., Sekine, M., Baba, S., Kosugi, H., Hosoyama, A., Nagai, Y., Sakai, M., Ogura, K., Otuka, R., Nakazawa, H., Takamiya, M., Ohfuku, Y., Funahashi, T., Tanaka, T., Kudoh, Y., Yamazaki, J., Kushida, N., Oguchi, A., Aoki, K., Nakamura, Y., Robb, T. F., Horikoshi, K., Masuchi, Y., Shizuya, H., and Kikuchi, H. (1998) *DNA Res.* **5,** 55–76
23. Watanabe, F., Abe, K., Tamura, Y., and Nakano, Y. (1996) *Microbiology* **142,** 2631–2634
24. Holloway, D. E., and Marsh, E. N. G. (1994) *J. Biol. Chem.* **269,** 20425–20430
25. Chen, H. P., and Marsh, E. N. G. (1997) *Biochemistry* **36,** 14939–14945
26. Kellermeyer, R. W., Allen, S. H. G., Stjernholm, R., and Wood, H. G. (1964) *J. Biol. Chem.* **239,** 2562–2569
27. Tollinger, M., Konrat, R., Hilbert, B. H., Marsh, E. N. G., and Krautler, B. (1998) *Structure* **6,** 1021–1033
28. Thoma, N. H., Meier, T. W., Evans, P. R., and Leadlay, P. F. (1998) *Biochemistry* **37,** 14386–14393